Analyst

PAPER

View Article Online
View Journal | View Issue

Cite this: *Analyst*, 2014, **139**, 4855

A rapid method to estimate the concentration of citrate capped silver nanoparticles from UV-visible light spectra†

D. Paramelle,[a] A. Sadovoy,*[a] S. Gorelik,[a] P. Free,*[a] J. Hobley[a] and D. G. Fernig[b]

Received 29th May 2014
Accepted 1st July 2014

DOI: 10.1039/c4an00978a

www.rsc.org/analyst

We present a generalized table of extinction coefficient data for silver nanoparticles from 8 to 100 nm. This table allows for easy and quick estimation of the concentration and size of modified and mono-dispersed silver nanoparticles from their optical spectra. We obtained data by determining the silver content of citrate-stabilised silver nanoparticles using sodium cyanide to dissolve the nanoparticles, and measuring solution conductivity with a pH meter and a cyanide-ion selective electrode. The quantification of the silver ion concentration enabled the calculation of extinction coefficients. Experimentally calculated extinction coefficients, in the current work, are in good agreement with collated literature values measured by different authors with non-standardized methodology and each for a limited range of particle size. They are also in good agreement with our theoretical calculations using Mie theory. Thus, we provide a highly standardized and comprehensive tabulated reference data-set.

Introduction

The popularity of noble metal nanoparticles as sensors is in part due to their highly sensitive colorimetric properties. The red or yellow colour of gold or silver nanoparticles, respectively, is obvious to the naked eye, even at picomolar concentrations. The aggregation assay of gold nanoparticles, whereby the nanoparticles interact with each other when a designed sensor interaction is introduced, is seen as a red to purple colour change in the nanoparticle solution.[1,2] The strong colour identity of gold and silver nanoparticles results from their strong absorption and scattering of light. Silver nanoparticles are both visually and spectroscopically detectable at lower concentration than gold nanoparticles and there are several studies that demonstrate the facile use of silver nanoparticles as biosensors.[3–12] Their application as colorimetric biosensors is intrinsically linked to particle size, extinction efficiency, and concentration. However, unfortunately, a simply and quick way to estimate these three parameters does not exist. Recently tabulated data for determining the concentration of uncoated spherical gold nanoparticles in water from UV-vis spectra in a wide range of sizes were published.[13] This data have provided a valuable reference source in the field of gold nanoparticles. With such a table for silver nanoparticles it would be easy to calculate the concentration. Despite some reports existing for extinction coefficients of silver nanoparticles,[14–18] there is clearly a need for a comprehensive table of data that will allow many scientists to use silver nanoparticles easily in quantitative experiments.

Current methods to determine the concentration of metal nanoparticles require knowing the nanoparticle size (typically by transmission electron microscopy – TEM) and knowing the amount of metal atoms in the colloidal sample. This latter step often requires using specialized, very expensive and time consuming equipment, such as asymmetric flow field fractionation or inductively coupled plasma mass spectroscopy,[19–23] which is destructive to the sample. In contrast, rapid optical methods for determining the concentration of nanoparticles, if available, could be performed routinely at each step of sample preparation. This would allow, for instance, the monitoring of passivation,[24–26] as well as the degradation of a sample of nanoparticles over time through aggregation. The potential of an optical quantification method is demonstrated by the great popularity of the data published for gold nanoparticles with, to date, greater than 300 citations.[13]

Here, we present a table of generalized data for silver nanoparticles, generated with a parallel control experiment for gold nanoparticles for reference. To obtain these data we develop a method to determine the amount of silver or gold ion content from citrate-coated nanoparticle solutions dissolved with sodium cyanide. The consumption of cyanide is measured by recording the change in conductance of the solution using a pH meter and a cyanide-ion selective electrode. Silver

[a]*Institute of Materials Research and Engineering, A*STAR (Agency for Science, Technology and Research), 3 Research Link, Singapore 117602. E-mail: sadovoya@imre.a-star.edu.sg; freepf@imre.a-star.edu.sg*

[b]*Department of Biochemistry, Institute of Integrative Biology, University of Liverpool, Liverpool L69 7ZB, UK*

† Electronic supplementary information (ESI) available: Extra figures, definitions and HR-TEM images. A table of extinction coefficients of citrate-capped silver nanoparticles for calculating nanoparticle concentrations. See DOI: 10.1039/c4an00978a

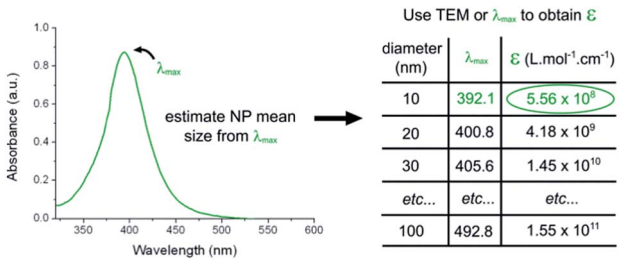

Scheme 1 Calculation of the silver nanoparticle concentration. The extinction coefficient of citrate-coated nanoparticles can be calculated using Table S1† and the diameter of the nanoparticles estimated by λ_{max} or by TEM.

nanoparticles are dissolved to form the expected $[NaAgCN_2]$ complex. The method developed was also verified on the reference control gold nanoparticles. From the known absorbance of solutions of silver nanoparticles of different sizes (as determined by high-resolution (HR) TEM), extinction coefficients were derived at the maximum absorbance in the UV-vis spectrum for citrate-stabilized spherical silver nanoparticles (Scheme 1).

These data were comparable with data found in the literature. Extinction coefficients were calculated independently using Mie theory and correlate well with the experimental data. Thus, our approach provides a rapid means to estimate the size, concentration, and molar decadic extinction coefficient of spherical silver nanoparticles using a generalized table.

Experimental

Safety note

The use of cyanide salts must be done under alkaline conditions, using a 0.1 M NaOH solution, for instance, in order to avoid the production of highly toxic HCN gas.

Materials

Citrate-coated colloidal silver nanoparticles were purchased from nanoComposix Inc. (CA, USA). Sodium hydroxide, sodium cyanide, nitric acid and sulphuric acid were obtained from Sigma Aldrich Pte Ltd (Singapore). All reagents were used as supplied. Nanosep 30 kDa filters were purchased from VWR Pte Ltd (Pall Inc, USA).

Titration of sodium cyanide standard

Ten dilutions of sodium cyanide (final concentration between 0.1 mM and 1 mM in steps of 0.1 mM) in 0.1 M NaOH solution were prepared freshly on each day of experimentation. For each sample, free cyanide ion content was measured using an OR Ionplus Sure-Flow cyanide ion selective electrode and an Orion 5 Star pH meter (Thermo Fisher Scientific, Singapore). Electrode potential recordings were taken once the electrode potential value stabilized. A sodium cyanide calibration curve (Fig. S1†) was obtained from which fitting to the Nernst equation allowed the free cyanide ion content to be calculated. The cyanide ion selective electrode does not detect gold or silver complexed cyanide.[27]

UV-visible spectroscopy

UV-visible spectra were recorded at room temperature using a Molecular Probes (Oregon, USA) Spectramax 384-well spectrometer, using a 1 cm path length quartz cuvette, and a fixed slit width of 2 nm. The spectrometer was calibrated daily using the machine's 'Auto-Calibrate' air calibration. Baseline calibration to zero can be performed at 1000 nm if baseline drift is observed, however we did not do this correction as all spectra satisfactory approximated to zero at 1000 nm. Comparative standard spectra were recorded using a Shimadzu UV-3600 (2 nm slit width) and an Ocean Optics USB-4000 with 1.5 nm per pixel resolution (Fig. S15†). Using the same spectrometer and quartz cuvette is recommended.

Determination of nanoparticle absorbance of cyanide-treated stock

Colloidal gold or silver nanoparticles of different volumes (between 5–18 mL per sample) were concentrated to 1.2 mL volume by centrifugation for 90 min at a speed that was appropriate to softly pellet the nanoparticles. For example, 40 nm and 50 nm gold or silver nanoparticles were centrifuged at 1000 rcf, whereas 10 nm gold or silver nanoparticles were centrifuged at 15 000 rcf. One mL was used for cyanide treatment, while 200 μL of these nanoparticles were used for absorbance measurements. UV-visible spectroscopy was performed between 320 nm and 1000 nm (450–750 nm for gold) at an appropriate dilution whereby the absorbance at the λ_{max} was between 0.3 and 0.4 (silver nanoparticles $\leq$ 50 nm) or lower than 0.3 (silver nanoparticles > 50 nm). For gold nanoparticles an absorbance below 0.7 at 450 nm was used. The sample blank was obtained from this solution by filtering the nanoparticles using NanoSep 30 kDa cutoff filters.

HR-TEM of silver nanoparticles

Silver nanoparticles were concentrated by ultrafiltration of stock solutions with Nanosep 30 kDa filters. Concentrated solutions were deposited on Ultrathin Carbon (<3 nm) on Carbon Holey support film TEM grids (400 mesh, Pelco International, USA). Silver nanoparticles were analysed with a Philips CM300 high resolution analytical TEM/STEM. Obtained images were not digitally modified, such as, for example, to remove the carbon grids. Measurements of the metal core of the nanoparticles of different sizes were done with different magnifications to provide similar resolution, *i.e.*, ratio of the size of the pixel and the diameter of the nanoparticle was kept constant. In general, this ratio was kept to 15, providing consistent accuracy of the metal core size measurement. The size determination of the metal core of nanoparticles and their circularity was carried out using ImageJ v1.47e software using a macro 'Particle Size Analyzer'. Data were expressed as %volume:

$$\%V_{\mathrm{tot}D} = (n \times D^3/\sum n \times \mathrm{Di}^3) \times 100$$

where D is the diameter of the nanoparticles, $\%V_{\mathrm{tot}D}$ is the percentage volume total of the nanoparticles with a diameter D,

and n is the TEM number count. The mean diameter of the metal core was estimated by log-normal distribution.

Dissolving nanoparticles with sodium cyanide

A 50 mL flask and stirrer bar were cleaned with *aqua regia* and washed with copious amounts of water and dried. Two mL of 10 mM sodium cyanide in 0.1 M sodium hydroxide was added to the 50 mL flask and stirred rapidly at 1000 rpm. One mL of concentrated nanoparticles was added slowly dropwise to the stirred sodium cyanide solution. If a brief colour change occurred, the next drop was not added until the solution returned colourless. After addition, the solution was continually stirred for a further 10 min. The stirring rate was decreased to 200 rpm, and 27 mL of 0.1 M NaOH was added. After a minute of mixing, the stirring was stopped, the cyanide ion selective electrode was placed in the solution and an electrode potential reading was taken. Four more electrode potential measurements were taken at total volumes of 35 mL, 40 mL, 45 mL and 50 mL (by addition of further volumes of 0.1 M NaOH). A population standard deviation from the calculated cyanide concentration of less than 10% (gold) or 12% (silver) was acceptable for nanoparticle concentration analysis.

Simulation of silver nanoparticle extinction

Simulations were performed by modification of the FORTRAN 77 code reported by Haiss *et al.*,[13] originally published by Bohren and Huffman.[28]

Results and discussion

Defining the problem involving the calculation of silver nanoparticle concentrations

The optical properties of silver nanoparticles can change depending on the size,[16,29] shape,[30–32] composition,[15] and surface capping[3,4,33–36] used to form monolayers around the nanoparticles. Within this manuscript we measured the HR-TEM and λ_{max} values of a series of commercially purchased citrate-capped silver nanoparticles, and compared these data with those obtained from the manufacturer (Table S2†). With the best efforts of ourselves and the manufacturer, it is clear from Table S2† that deviations in the data for the HR-TEM diameter and λ_{max} do occur. This will inevitably lead to variance in the calculation of the nanoparticle concentration.[11] We felt that a standardized set of parameters, such as an extinction coefficient or the λ_{max} value for a size of the nanoparticle, would allow the user to interpret their data to calculate nanoparticle concentrations using our standardised table data (Table S1†). Here we present our own quantification method for determining the nanoparticle concentration, and compare with literature and simulation data.

Quantification of dissolved noble metal nanoparticles with cyanide

The noble metal cyanide process is a major method for commercial extraction of silver or gold compounds from true ores.[37] The formation of highly water-soluble potassium dicyanoargentate(I) $[KAg(CN)_2]$ or potassium dicyanoaurate(I) $[KAu(CN)_2]$ (or equivalent sodium salts) is one of the steps in this process and involves the treatment of processed ores with aqueous potassium cyanide. The formation of insoluble silver cyanide(I) and gold cyanide(I) salts is also a part of the process, but these are dissolved well by aqueous potassium cyanide to form the dicyano salts.[37] Our hypothesis for the dissolution of noble metal nanoparticles by alkaline-metal cyanide salts was that, under favourable conditions, the formation of dicyano compounds $[xAgCN_2]$ or $[xAuCN_2]$ (x = Na or K) goes to completion, to yield a stoichiometric ratio of cyanide complex to noble metal of 2 : 1. To test this hypothesis, changes in the concentration of cyanide ions remaining after dissolving noble metal nanoparticles were measured with a highly sensitive cyanide ion-selective electrode. This allowed the determination of the amount of cyanide before and after adding nanoparticles, from a known stock concentration. Gold nanoparticles were chosen as the reference control, because the molar concentration is quantifiable from UV-visible absorbance spectra using published extinction coefficient data.[13] This allowed independent calculation of the expected cyanide to gold ratio. An important safety note is that cyanide salts must be used under alkaline conditions, using a 0.1 M NaOH solution for instance, in order to avoid the production of highly toxic HCN gas.

Several parameters were required in order to calculate changes in cyanide ion concentration upon dissolving the gold nanoparticles. To obtain a standard curve for CN^- *vs.* electrode potential, electrode potentials were recorded for a set of sodium cyanide concentrations in the range of use for the dissolution experiment (0–1 mM), using a cyanide ion-selective electrode at room temperature. The data fitted well to the Nernst equation (Fig. S1†). Samples of citrate-stabilized gold nanoparticles for dissolution by cyanide were prepared by concentrating stock nanoparticles by centrifugation. UV-visible spectra of re-diluted samples in water showed no change in the particle spectra, suggesting that the concentrated sample remained stable against aggregation (data not shown). The nanoparticles were dissolved with sodium cyanide and diluted, so that electrode potential readings would fit into the standard curve range. The absorbance at 450 nm of a known dilution of the stock solutions allowed for the determination of the molar concentration of concentrated gold nanoparticles using data provided by Haiss *et al.*[13]

By considering the molar concentration of nanoparticles, volume, mass (ESI Definition S1†) and mean consumption of cyanide ions from five dilution measurements, the ratio of CN^- to gold was calculated for several different sizes of gold nanoparticles (Fig. 1). The average of these data points is a ratio of 1.91 ± 0.16, which equates to approximately 95% of the total gold content forming the dicyano gold salt $[NaAu(CN)_2]$. Note that monomeric or chains of gold–cyanide complexes[38] would have a molar ratio of ~1. All data recorded for this procedure before optimization of the conditions had a ratio of 1.94 ± 0.16 (Fig. S2†). Larger nanoparticles have values closer to 2.0 (Fig. 1). This correlates well with observations, as solutions of smaller nanoparticles had a fast, short lived (<1 s) colour change to

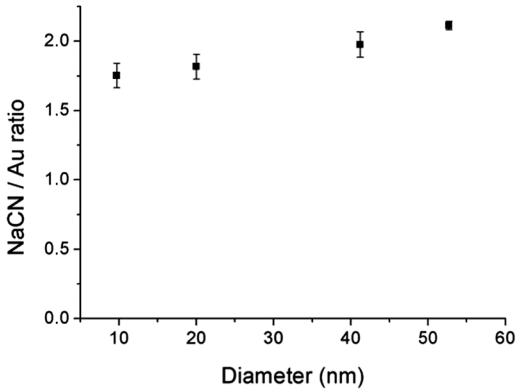

Fig. 1 Molar ratio of consumed sodium cyanide to gold for dissolved gold nanoparticles with mean sizes ranging from 9.4 nm to 52.7 nm. Data are the mean and standard deviation from three separate samples of different concentrations of nanoparticles.

purple before becoming colourless, possibly due to brief aggregation of the smaller nanoparticles.

Using the cyanide method to calculate the extinction coefficient of silver nanoparticles

In an analogous experiment to that with gold nanoparticles, citrate-stabilized spherical silver nanoparticles of different sizes, from 8.4 nm to 95.3 nm diameter, were concentrated and dissolved with cyanide. The mole consumption of silver (and subsequently of silver nanoparticles) is calculated from the known mole consumption of cyanide using a ratio of cyanide to silver of 1.91, as experimentally determined for gold. The Beer–Lambert law ($A = \varepsilon c d_0$) can then be used to calculate the molar decadic extinction coefficient from samples of known absorbance. Fig. 2 shows the mean experimental data and comparison with literature data. It is clear that our data fit well with those from the literature, however there is still some spread across our own and literature data, highlighting the need for a table of standardized extinction coefficient data for silver nanoparticles.

To ensure no bias in size data from the centrifugally concentrated samples, supernatants from centrifuged 10 nm and 30 nm silver nanoparticles were tested by the cyanide method to determine the silver content. Data comparing cyanide levels before and after addition of the supernatant suggested only a few percentage higher cyanide content after addition of the supernatant (not shown). Within the overall experimental error, we consider this to mean that there is a negligible amount of silver in the supernatants under the conditions we used for centrifugation. Moreover, the volume contribution of the smaller nanoparticles is very low, further validating the exclusion of small amounts of silver in the supernatant if present (Fig. S3†).

A boundary condition for the use of this method does exist; nanoparticles need to be fully dissolved by the use of sodium (or potassium) cyanide at the mentioned concentration (although higher concentrations could be used). This would certainly be the case for nanoparticles coated with citrate or tannic acid, and possibly polyvinylpyrolidine (although this has not been tested). Although it was not required here, the use of elevated temperatures would help in the dissolution process. We utilise our method with the very common citrate-capped nanoparticles. However, for using this method for samples with a different capping layer it would be important to achieve complete dissolution of silver to ensure accurate extinction coefficient estimation. It may, for example, prove more challenging with peptidol/alkane thiol ethylene glycol capped nanoparticles.[3]

Silver nanoparticle size and absorbance spectra characteristics

The spectra of silver nanoparticles are highly sensitive to particle size (Fig. 3 and S4†). The extinction coefficient of light is the net effect of scattering and absorption and describes the effect of the interaction between radiation and the matter upon

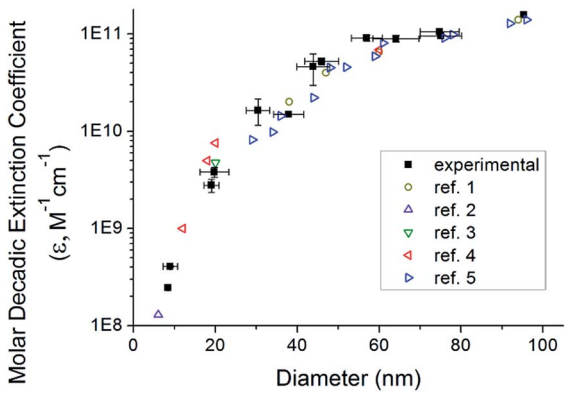

Fig. 2 Comparison of molar decadic extinction coefficients at absorbance at λ_{max} of experimental and literature data. The mean experimental data are plotted (black filled squares) with the x-error as diameter S.D. (determined from TEM), and the y-error as the standard error of data. Five different sets of literature data were included (all non-filled shapes): ref. 1 from Yguerabide *et al.*,[18] ref. 2 from Mulvaney *et al.*,[17] ref. 3 from Link *et al.*,[15] ref. 4 from Navarro *et al.*,[14] and ref. 5 from Evanoff *et al.*[16]

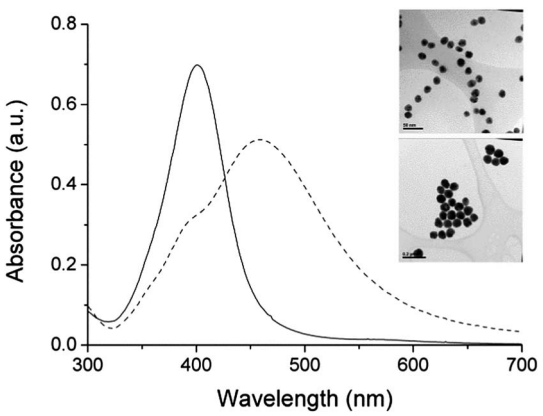

Fig. 3 UV-visible spectra and example HR-TEM images of 19.0 nm (solid line and upper image) and 74.8 nm (dashed line and lower image) citrate-capped silver nanoparticles. Larger sized HR-TEM images and histogram data are shown in Fig. S5b and S5j.†

which it impinges. In the case of silver nanoparticles, the volumetric cross-section plays a larger role in changing the spectra than for gold nanoparticles. This means that, for a population containing equal concentrations of two sizes of silver nanoparticles, the larger volume nanoparticles contribute more to the spectra or extinction coefficient value. As the diameter of nanoparticles is required for the calculations of their extinction coefficient, we used a volume-weighted distribution of diameter obtained by HR-TEM. The analysis of volume-weighted distribution instead of number-weighted distribution obtained by HR-TEM (Table S2†) gives a larger mean nanoparticle diameter (Fig. S3†). Example HR-TEM images for tested samples are shown in Fig. S5a–S5l.†

In addition to the extinction coefficient being influenced by the size, the contribution of the scattering to the extinction coefficient increases for larger silver nanoparticles. It is known that light absorbance of silver nanoparticles determined from the Beer–Lambert law is very accurate in diluted samples, where the multiple light scattering effect is minimal. At 52 nm the scattering and absorbance effects have similar contributions.[16] To define optimal concentrations of a sample at approximately 50 nm or lower, we did a series of absorption spectra measurements with different dilutions of 45.9 nm silver nanoparticles and compared this with simulated absorbance (Fig. S6†). An overlap of absorbance intensity for the maximum peak was found between absorbances of 0.3 and 0.4. Therefore, this range was chosen for absorbance measurements of silver nanoparticle dilutions of size 50 nm or lower.

Larger nanoparticles have a more pronounced scattering effect. Good linear fitting of sample dilution *vs.* absorbance was obtained below 0.3 of absorbance for larger nanoparticles (Fig. S7†). Hence, absorbance values below 0.3 were chosen for nanoparticles larger than 50 nm.‡ Using 50 nm and 80 nm silver nanoparticles, the spectrometer (Molecular Probes Spectramax 384) absorbance (below 0.3) was validated against two other spectrometers; Shimadzu UV-3600 (2 nm slit width) and Ocean Optics USB-4000 (no slit setting, but with a resolution of 1.5 nm per pixel). Five different samples prepared on different days gave an absorbance S.D. of 5.8%. Using the Spectramax 384 for calibration of Methylene Blue in water gave a peak extinction coefficient of $(7.34 \pm 0.11) \times 10^4$ M^{-1} cm^{-1} from three separate dilutions, comparable to the average values from a range of literature reports.[39–42]

Modelling extinction efficiency of silver nanoparticles

To support the experimental data for calculating the molar decadic extinction coefficient (ε) of silver nanoparticles described in previous sections, we used algorithms published by Haiss *et al.*[13] to compute the extinction efficiency of silver nanoparticles. The simulation of silver nanoparticles has been dealt with in the literature, so for brevity is discussed in the ESI as Definition S2.† In short, we used silver dielectric data published by Palik[43] and appropriate selection of optical constants for the development of simulated extinction data.

Comparison of experimental and simulated extinction coefficient

Here, comparison of experimental data and manufacturer supplied data of absorption peaks with simulated data by Mie theory for silver nanoparticles from 5 nm to 100 nm is shown in Fig. 4. Experimentally observed absorption peaks for particles in the 20–100 nm range are in good correlation with the simulation, though increasing the nanoparticle size gives a slight red shift due to larger nanoparticles contributing more towards absorbance and scattering (Fig. S13†). Also they are well interpolated with a quadratic function $= a + bx^2$ ($a = 397$; $b = 9.58 \times 10^{-3}$). Nanoparticles with diameters smaller than 20 nm have lower absorption peaks than simulated, which has also been demonstrated for gold nanoparticles.[13]

Fig. 5 shows the comparison of molar extinction coefficients for various sizes of silver nanoparticles obtained experimentally, determined from manufacturer supplied data, and simulated data. The agreement between experiment and simulation allows these data to be used to calculate the extinction coefficient for spherical citrate-stabilized silver nanoparticles over a wide range of diameters (Table S1†). This enables ready calculation of the concentration of silver nanoparticles from absorbance data in a non-destructive way. Obtained data were extrapolated in size ranges from 10 nm to 30 nm and from 30 nm to 100 nm by an exponential function $y = y_0 + A\exp(Rx)$ ($y_0 = -1.423 \times 10^9$, $A = 6.984 \times 10^8$ and $R = 0.104$) and a linear function $y = a + kx$ ($a = -4.709 \times 10^{10}$ and $k = 2.017 \times 10^9$), respectively.

Our calculation of the nanoparticle size was we assume correctly based upon the volume-weighted distribution of HR-TEM nanoparticle sizes, and not number-weighted distribution. We also calculated the size of nanoparticles and extinction coefficients using HR-TEM number-weighted distribution (ESI Fig. S14†) and found that there is only a small difference between the data, but note that sizes lower than 20 nm would be

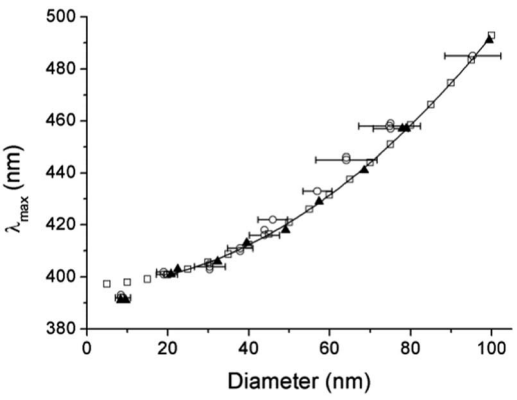

Fig. 4 Absorbance peaks for silver nanoparticles obtained experimentally (empty circles), manufacturer supplied information (black triangles) and simulated (empty squares). The *x*-error is the S.D. of the diameter.

‡ Zook *et al.*[47] suggest that the integrated area is a more accurate assessment of concentration than λ_{max}. We discuss this in ESI Fig. S8.†

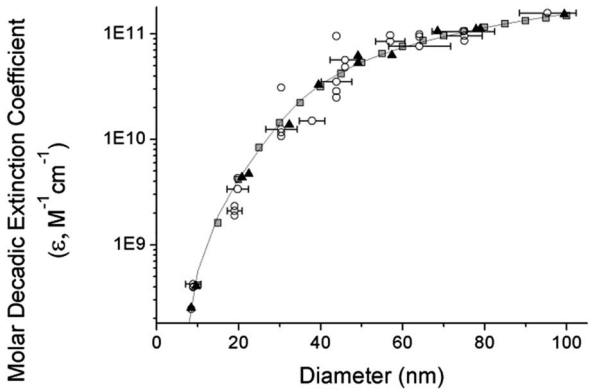

Fig. 5 Molar decadic extinction coefficient (ε) for silver nanoparticles. Data obtained experimentally (empty circles, selected points show the *x*-error as size S.D. determined from HR-TEM), obtained from manufacturer supplied information (black triangle), and simulated data (grey squares).

more accurately represented if the TEM size is expressed as a volume-weighted distribution. As some size histogram data looked asymmetric (Fig. S5a–S5l†), the mean diameters of the metal cores were estimated by a log-normal distribution. Estimation by Gaussian fit gave a smaller mean size difference of less than 0.3% (less than 0.7% for 8.9 nm silver).

A summary of some of the accumulated approximated data for spherical citrate-capped silver nanoparticles is shown in Table 1, with a full table presented in Table S1.†

Real silver nanoparticles have a size distribution typically up to ±5%, and thus can have a λ_{max} bias towards higher wavelengths due to larger nanoparticles contributing more towards absorbance and scattering. This is demonstrated in Fig. S13,† comparing simulated and experimental data of 75 nm spherical citrate-capped silver nanoparticles. From the table data, ε can be used to calculate the particle molar concentration c in mole per litre from the absorption A at the particles measured λ_{max}, using the Beer–Lambert law ($c = A/\varepsilon d_0$).

It should be noted that in addition to the size, changing the capping layer of silver nanoparticles will change their absorbance characteristics.[3,4,44–46] Therefore, under these circumstances the quantification of silver should be repeated. Alternatively, with care taken that the new capping layer does not result in loss of nanoparticles or their agglomeration, the absorbance spectrum of the capped nanoparticles can be directly calibrated against that of the starting nanoparticles to calculate a new extinction coefficient.

Table 1 Summary of the simulated data for λ_{max} and molar extinction coefficient of various sizes of citrate-capped silver nanoparticles

d/nm	λ_{max}/nm	ε/M^{-1} cm^{-1} × 10^8
10	392.1	5.56
20	400.8	41.8
30	405.6	145
40	412.3	336
50	420.9	537
60	431.5	739
70	443.8	941
80	458.3	1142
90	474.6	1344
100	492.8	1546

Conclusions

In this study, we provide useful information for all scientists involved in the use of colloidal solutions of spherical silver nanoparticles in the 8 to 100 nm size range and where the molar concentration of nanoparticles is needed such as in quantitative analysis. We first demonstrated a new method for the calculation of extinction coefficients for spherical silver nanoparticles. The method uses sodium cyanide to dissolve silver nanoparticles. Such treatment was expected to form divalent cyanide noble metal complexes [$NaXCN_2$] (X = noble metal), and we validated this against gold nanoparticles where extinction coefficients are known.[13] Obtained extinction coefficients for silver nanoparticles were compared against the literature and were shown to fit well. Using simple Mie theory for spherical silver nanoparticles, extinction coefficients were obtained and found to be in excellent agreement with experimental data and data provided by the nanoparticle manufacturer. Thus this study allowed the preparation of a complete table of extinction coefficient *vs.* nanoparticle size *vs.* theoretical nanoparticle λ_{max} wavelength. Importantly, this table provides a simple means for the calculation of citrate-capped silver nanoparticle concentrations of a wide range of sizes from their corresponding extinction coefficient. This is also applicable to the measurement of the concentration of silver nanoparticles during the assembly of new capping layers and their functionalization, either by measuring the silver content directly or by measuring the absorbance characteristics of the nanoparticles and calibrating this to those of the starting material.

Acknowledgements

This work has been supported by the Agency for Science, Technology and Research (A*STAR) (DP, AS, SG, PF, JH) as JCO Grant no. 10/03/FG/06/04, and DGF acknowledges the support of the North West Cancer Research Fund.

Notes and references

1 C. A. Mirkin, R. L. Letsinger, R. C. Mucic and J. J. Storhoff, *Nature*, 1996, **382**, 607–609.
2 P. A. Alivisatos, K. P. Johnsson, X. Peng, T. E. Wilson, C. J. Loweth, M. P. Bruchez Jr and P. G. Schultz, *Nature*, 1996, **382**, 609–611.
3 P. Free, D. Paramelle, M. Bosman, J. Hobley and D. G. Fernig, *Aust. J. Chem.*, 2012, **65**, 275–282.
4 R. C. Doty, T. R. Tshikhudo, M. Brust and D. G. Fernig, *Chem. Mater.*, 2005, **17**, 4630–4635.
5 J. Wrzesien and D. Graham, *Tetrahedron*, 2012, **68**, 1230–1240.

6 L. R. Skewis and B. M. Reinhard, *ACS Appl. Mater. Interfaces*, 2010, **2**, 35–40.
7 X. Xu, J. Wang, F. Yang, K. Jiao and X. Yang, *Small*, 2009, **5**, 2669–2672.
8 A. Steinbrück, A. Csaki, K. Ritter, M. Leich, J. M. Köhler and W. Fritzsche, *J. Biophotonics*, 2008, **1**, 104–113.
9 J. Zhang, J. Malicka, I. Gryczynski and J. R. Lakowicz, *Anal. Biochem.*, 2004, **330**, 81–86.
10 B. C. Vidal, Jr, T. C. Deivaraj, J. Yang, H.-P. Too, G.-M. Chow, L. M. Gan and J. Y. Lee, *New J. Chem.*, 2005, **29**, 812–816.
11 J.-S. Lee, A. K. R. Lytton-Jean, S. J. Hurst and C. A. Mirkin, *Nano Lett.*, 2007, **7**, 2112–2115.
12 K. Aslan, P. Holley and C. D. Geddes, *J. Mater. Chem.*, 2006, **16**, 2846.
13 W. Haiss, N. T. K. Thanh, J. Aveyard and D. G. Fernig, *Anal. Chem.*, 2007, **79**, 4215–4221.
14 J. R. G. Navarro and M. H. V Werts, *Analyst*, 2013, **138**, 583–592.
15 S. Link, Z. L. Wang and M. a. El-Sayed, *J. Phys. Chem. B*, 1999, **103**, 3529–3533.
16 D. D. Evanoff and G. Chumanov, *J. Phys. Chem. B*, 2004, **108**, 13957–13962.
17 P. Mulvaney, M. Giersig and A. Henglein, *J. Phys. Chem.*, 1993, **97**, 7061–7064.
18 J. Yguerabide and E. E. Yguerabide, *Anal. Biochem.*, 1998, **262**, 157–176.
19 E. Bolea, J. Jiménez-Lamana, F. Laborda and J. R. Castillo, *Anal. Bioanal. Chem.*, 2011, **401**, 2723–2732.
20 A. Hahn, J. Fuhlrott, A. Loos and S. Barcikowski, *J. Nanopart. Res.*, 2012, **14**, 1–10.
21 S. Gschwind, H. Hagendorfer, D. A. Frick and D. Gu, *Anal. Chem.*, 2013, **85**, 5875–5883.
22 Method used for analysis of nanoparticles by the silver nanoparticle manufacturer Nanocomposix Inc, http://www.nanocomposix.com, accessed May 2014.
23 T. Shamspur, M. H. Mashhadizadeh and I. Sheikhshoaie, *J. Anal. At. Spectrom.*, 2003, **18**, 1407–1410.
24 M. J. Hostetler, A. C. Templeton and R. W. Murray, *Langmuir*, 1999, **15**, 3782–3789.
25 X. Chen, W. W. Qoutah, P. Free, J. Hobley, D. G. Fernig and D. Paramelle, *Aust. J. Chem.*, 2012, **65**, 266–274.
26 L. Duchesne, D. Gentili, M. Comes-Franchini and D. G. Fernig, *Langmuir*, 2008, 13572–13580.
27 *User guide – cyanide ion selective electrode*, Thermo Fisher Scientific, Rev. A 12–08.
28 C. F. Bohren and D. R. Huffman, *Absorption and Scattering of Light by Small Particles*, Wiley-VCH Verlag GmbH, Weinheim, Germany, 1998.
29 D. C. Skillman and C. R. Berry, *J. Opt. Soc. Am.*, 1973, **63**, 707–713.
30 E. A. Coronado and G. C. Schatz, *J. Chem. Phys.*, 2003, **119**, 3926–3933.
31 J. A. Creighton and D. G. Eadon, *J. Chem. Soc., Faraday Trans.*, 1991, **87**, 3881–3891.
32 N. R. Jana, L. Gearheart and C. J. Murphy, *Chem. Commun.*, 2001, 617–618.
33 J. A. Adekoya, E. O. Dare, K. O. Ogunniran, T. O. Siyanbola, A. A. Akinsiku, C. O. Ehi-, C. O. Ajanaku and W. U. Anake, *Int. J. Sci. Eng. Res.*, 2014, **5**, 1220–1226.
34 S. He, J. Yao, P. Jiang, D. Shi, H. Zhang, S. Xie, S. Pang and H. Gao, *Langmuir*, 2001, **17**, 1571–1575.
35 S. Bhat and U. Maitra, *J. Chem. Sci.*, 2009, **120**, 507–513.
36 A. Stewart, S. Zheng, M. R. McCourt and S. E. J. Bell, *ACS Nano*, 2012, **6**, 3718–3726.
37 A. N. B. Rumby, U. Ag, C. Kg, P. E. B. Raumann, K. L. Z. Immermann, F. R. V An, D. E. N. B. Roeck, P. E. T. Ews, R. Allgem, S. Agosi, B. E. K. Empf, C. A. P. Eter and K. Der, in *Ullman's Encyclopedia of Industrial Chemistry*, Friedrich-schiller-universit, Wiley-VCH Verlag GmbH & Co. KGaA, Weinheim, Germany, 2000.
38 G. A. Bowmaker, B. J. Kennedy and J. C. Reid, *Inorg. Chem.*, 1998, **37**, 3968–3974.
39 K. Bergmann and C. T. O'Konski, *J. Phys. Chem.*, 1963, **67**, 2169–2177.
40 C. Kaewprasit, E. Hequet, N. Abidi and J. P. Gourlot, *J. Cotton Sci.*, 1998, **2**, 164–173.
41 S. Prahl, Oregon Medical Laser Center, Optical Absorption of Methylene Blue, http://omlc.ogi.edu/spectra/mb/index.html, accessed May 2014.
42 T. Mahmood, F. Anwer, I. Mahmood, F. Kishwar and A. Wahab, *Eur. Acad. Res.*, 2013, **I**, 1100–1109.
43 *Handbook of Optical Constants of Solids*, ed. E. D. Palik, Academic Press, New York, 1985.
44 O. Tzhayik, P. Sawant, S. Efrima, E. Kovalev and J. T. Klug, *Langmuir*, 2002, **18**, 3364–3369.
45 T. Ung, L. M. Liz-Marzán and P. Mulvaney, *Langmuir*, 1998, **14**, 3740–3748.
46 N. G. Bastús, F. Merkoçi, J. Piella and V. Puntes, *Chem. Mater.*, 2014, **26**, 2836–2846.
47 J. M. Zook, S. E. Long, D. Cleveland, C. L. a. Geronimo and R. I. MacCuspie, *Anal. Bioanal. Chem.*, 2011, **401**, 1993–2002.